PROCEEDINGS OF SCIENCE

Nuclear astrophysics studies with indirect methods

C.A. Bertulani[*†]
Department of Physics and Astronomy, Texas A&M University, Commerce, TX 75429, USA
E-mail: carlos_bertulani@tamu-commerce.edu

We observe photons and neutrinos from stars. Based on these observations, complemented by measurements of cosmic rays energies and composition, we have been able to constrain several models for the Big Bang and for stellar evolution. But that is not enough. We also need to help this effort with laboratory experiments. We are still far from being able to reproduce stellar environments in a terrestrial laboratory. But in many cases we can obtain accurate nuclear reaction rates needed for modeling primordial nucleosynthesis and hydrostatic burning in stars. The relevant reactions are difficult to measure directly in the laboratory at the small astrophysical energies. In recent years indirect reaction methods have been developed and applied to extract low-energy astrophysical S-factors. These methods require a combination of new experimental techniques and theoretical efforts, which are the subject of this short review.

VI European Summer School on Experimental Nuclear Astrophysics, ENAS 6
September 18-27, 2011
Acireale Italy

[*]Speaker.

[†]This work was supported by the US Department of Energy grants DE-FG02-08ER41533 and DE-FG02-10ER41706.

PoS(ENAS 6)023

1. Astrophysics: what we can and what we can't do

Evidently, we cannot reproduce in the laboratory conditions existing during the Big Bang and during stellar evolution. But efforts to reproduce such conditions on a limited scale on Earth are underway. A good example are experiments being carried out at the National Ignition Facility (NIF) in Livermore. In this facility the intense energy of 192 giant laser beams is focused on a small spherical pellet containing a few milligrams of fusion fuel, typically a mix of deuterium and tritium. The energy heats the surface of the pellet into a plasma, exploding off its surface, driving the remaining portion of the target inwards, and compressing it into a high density. A shock wave travels towards the center of the compressed fuel from all sides, further heating and compressing it so that fusion reactions will occur and release energy, creating temperatures and pressures similar to those that exist only in the cores of stars and giant planets and inside nuclear weapons [1].

Another example is ITER, a large-scale international laboratory located in France that aims to demonstrate that it is possible to produce commercial energy from fusion. ITER is based on the "tokamak" concept of magnetic confinement, in which the plasma is contained in a doughnut-shaped vacuum vessel. A mixture of deuterium and tritium is heated to temperatures of 150 million $^{\circ}$C, forming a hot plasma. Strong magnetic fields are used to keep the plasma away from the walls. From 50 MW of input power, the ITER machine is designed to produce 500 MW of fusion power. ITER runs on a predicted 15 billion euros building cost, whereas NIF already costs roughly US$ 5 billions. So, these are not cheap machines at all. It is very hard to reproduce conditions within stars. And the prospects of generating energy for commercial use with similar projects in the future are still uncertain. As for helping us understanding features of the Big Bang and of stellar evolution, ITER will not be able to tell us much. It will mainly access questions on atomic and material science associated with confining a plasma at huge temperatures within a vessel and the interactions of the plasma with the walls of the vessel. While it is undeniable that this experiment will fill a knowledge gap needed for further developments in science, it will not answer crucial questions of relevance for astrophysics [2]. Maybe ITER-2 will, if we can afford it.

To avoid sounding too negative, I mention that NIF has a good plan to provide results on atomic and nuclear physics for stellar evolution. I give a couple of examples. In the theoretical modeling of stellar evolution one relies strongly on calculations of radiation propagation through hot stellar plasmas. The coefficient entering the radiation propagation equation is called the "opacity". It accounts for the interaction of photons with atoms and effects such as excitation and ionization of ground-state, excited, or ionized atomic species present in the medium. For many years we have relied on a huge effort to calculate all of the atomic physics needed for stellar evolution codes in the form of opacity tables [3]. Stellar modelers have not questioned much the reliability of such tables, as one simply can't do better than that. But it would be a great knowledge improvement if we could effectively "measure" opacity in the laboratory. The NIF X-ray opacity platform will enable detailed studies of the radiative properties of hot dense matter over a photon energy range of 200 - 10,000 eV, also important in astrophysics [4]. It will allow benchmarking opacities used in the standard solar model and in stellar equilibrium codes (relevant to exoplanet habitability assessment) and absorption/emission spectroscopy of photoionized plasmas scaled to black hole and neutron star accretion-disk conditions. The development of pulsed power and high power lasers opens a brand new perspective for the study of opacities in several dense plasmas including

modeling of the atmospheres of very cool white dwarf stars [5].

2. Nuclear reactions

Stars are powered by nuclear reactions at very low energies and, in many situations, at very high densities. Usually, one needs to know what happens during binary encounters between nuclei (a counter-example is the celebrated triple-α reaction). The effects of the environment electrons are still a disputed research topic. But the main problem here is really to know the reaction rates at the energies required for stellar modeling. For example, in our Sun the reaction ^{7}Be$(p,\gamma)^8$B plays a major role for the production of high energy neutrinos from the β-decay of ^{8}B. These neutrinos come directly from the center of the Sun and are ideal probes of the sun's structure. John Bahcall frequently said that this was the most important reaction in nuclear astrophysics [6]. Our knowledge about this reaction has improved considerably due to new radioactive beam facilities. Another example, the reaction $^{12}C(\alpha,\gamma)^{16}O$, is extremely relevant for the fate of massive stars. It determines if the remnant of a supernova explosion becomes a black-hole or a neutron star. These two reactions are just two examples of a large number of reactions which are not yet known with the required accuracy needed in astrophysics.

NIF has reported the first cross section and spectral measurements of the T(t,2n)^{4}He reaction that is an important mirror reaction to the ^{3}He(^{3}He,2p)^{4}He reaction (which is part of the proton-proton chain in hydrogen burning stars). These direct measurements, which were conducted at energies inaccessible by conventional accelerator-based techniques, are not affected by electron screening. Measurements of the differential cross section for the elastic n-^{3}H and n-^{2}H scattering at 14.1 MeV have also been published [7]. The accurate determination of this reaction rate is essential for understanding how the fuel is assembled in an implosion, and for the demonstration of thermonuclear ignition and net energy gain at NIF. It also opens the door for planning the use of NIF and other laser powered facilities to obtain information on nuclear reaction rates at the energies occurring in stars.

The extremely low cross sections for reactions induced by charged particles and the inherent difficulty to obtaining reaction cross sections induced by low energy neutrons leads to enormous hurdles to develop reliable stellar evolution models and computer codes. Chains of low energy nuclear reactions lead to complicated phenomena such as nucleosynthesis, supernovae explosions, and energy production in stars. An example is that approximately half of all stable nuclei observed in nature in the heavy element region, $A > 60$, are produced during the "r–process". The exact site of the r–process is not known, but one believes that it occurs in environments with large neutron densities leading to neutron capture times much smaller than the beta-decay half–lives, $\tau_n \ll \tau_\beta$, of the nuclei involved. The most neutron–rich isotopes along the r–process path have lifetimes of less than one second; typically 10^{-2} to 10^{-1} s. Cross sections for most of the nuclei involved are hard to measure experimentally. Sometimes, theoretical calculations of the capture cross sections and of the beta–decay half–lives are the only source of input for r–process modeling.

Nucleosynthesis in stars is also complicated by the presence of electrons. They screen the nuclear charges, therefore increasing the fusion probability by reducing the Coulomb repulsion. Evidently, the fusion cross sections measured in the laboratory have to be corrected by the electron

screening when used in a stellar model. This is a purely theoretical problem as one can not exactly reproduce the conditions at stellar interiors in the laboratory. At least for now.

A simpler screening mechanism occurs in laboratory experiments due to the bound atomic electrons in the nuclear targets. This case has been studied in great detail experimentally, as one can control different charge states of the projectile+target system in the laboratory [8, 9, 10, 11, 12]. The experimental findings disagree systematically by a factor of two or more with theory. This is surprising as the theory for atomic screening in the laboratory relies on our basic knowledge of atomic physics. At very low energies one can use the simple adiabatic model in which the atomic electrons rapidly adjust their orbits to the relative motion between the nuclei prior to the fusion process. Energy conservation requires that the larger electronic binding (due to a larger charge of the combined system) leads to an increase of the relative motion between the nuclei, thus increasing the fusion cross section. As a matter of fact, this enhancement has been observed experimentally. The measured values are however not compatible with the adiabatic estimate [8, 9, 10, 11, 12]. Dynamical calculations have been performed, but they obviously cannot explain the discrepancy as they include atomic excitations and ionizations which reduce the energy available for fusion. Other small effects, like vacuum polarization, atomic and nuclear polarizabilities, relativistic effects, etc., have also been considered [13]. But the discrepancy between experiment and theory remains [13, 10].

A possible solution of the laboratory screening problem was proposed [14, 15]. Experimentalists often use the extrapolation of stopping power tables [16] to obtain the average value of the projectile energy due to stopping in the target material. The stopping is due to ionization, electron-exchange, and other atomic mechanisms. However, the extrapolation is challenged by theoretical calculations which predict a lower stopping. Smaller stopping was indeed verified experimentally [10]. At very low energies, it is thought that the stopping mechanism is mainly due to electron exchange between projectile and target. This has been studied in Ref. [17] in the simplest possible situation: proton+hydrogen collisions. The calculated stopping power was added to the nuclear stopping power mechanism, i.e. to the energy loss by the Coulomb repulsion between the nuclei. The obtained stopping power is proportional to v^{α}, where v is the projectile velocity and $\alpha = 1.35$. The extrapolations from stopping power tables predict a smaller value of α. Although this result seems to indicate the stopping mechanism as a possible reason for the laboratory screening problem, the theoretical calculations tend to disagree on the power of v at low energy collisions [18].

Another calculation of the stopping power in atomic He^{+}+He collisions using the two-center molecular orbital basis was reported in Ref. [19]. The agreement with the data from Ref. [18] at low energies is excellent. The agreement with the data disappears if nuclear recoil is included. In fact, the unexpected “disappearance" of the nuclear recoil was also observed in Ref. [20]. This seems to violate a basic principle of nature, as the nuclear recoil is due to Coulomb repulsion between projectile and target atoms [16]. After several attempts, sometimes with elaborate theoretical models, little theory activity in this field has been reported. Some models have been praised as solving the stellar screening problem (see, e.g. [21]). But the fact is that the present situation on screening of nuclear reactions is confusing. Either experimentalists are publishing wrong analysis, or all aspects of theory might not have been considered yet [22].

I have discussed above a few ongoing efforts in nuclear astrophysics, some expensive invest-

ments to get solutions, as well as some problems that might not even be possible to study on Earth. Actually, much of the knowledge required for understanding the physics of the Big Bang and of stellar evolution can be accessed by means of indirect methods in nuclear physics. The goal of these theoretical methods, and laboratories that use them, is to take a detour following a much harder work of putting pieces together from several, sometimes seemingly unrelated, experiments. In this article I will review some of these methods and what has been and can be accomplished with them.

2.1 Fusion

All approaches to understand fusion reactions involve two prongs: a) Calculate an ion-ion (usually one-dimensional) phenomenological potential (Wood-Saxon, proximity, folding, Bass, etc.) using frozen densities, or microscopic, macroscopic-microscopic methods using collective variables (CHF, ATDHF, empirical methods), and b) employ quantum mechanical tunneling methods for the reduced one-body problem (WKB, IWBC), incorporating quantum mechanical processes by hand, including neutron transfer and excitations of the entrance channel nuclei (CC) [23]. Only for very light ions, involving nuclei lighter than oxygen it is possible to devise more microscopic methods, based on binary nucleon-nucleon interactions, to obtain the fusion reaction cross sections of interest for nuclear astrophysics [24].

Fusion cross sections can be calculated from the equation

$$\sigma_F(E) = \pi\lambda^2 \sum_\ell (2\ell+1) P_\ell(E), \tag{2.1}$$

where E is the center of mass energy, $\lambda = \sqrt{\hbar^2/2mE}$ is the reduced wavelength and $\ell = 0, 1, 2, \cdots$. The cross section is proportional to $\pi\lambda^2$, the area of the quantum wave. Each part of the wave corresponds to different impact parameters having different probabilities for fusion. As the impact parameter increases, so does the angular momentum, hence the reason for the $2\ell+1$ term. $P_\ell(E)$ is the probability that fusion occurs at a given impact parameter, or angular momentum. The barrier penetration method (BPM) assumes that fusion occurs when the particle (with mass m) penetrates the Coulomb barrier and P_ℓ is calculated in a one-dimensional potential model, e.g. by using the WKB approximation or alike. From $\sigma_\ell = \pi\lambda^2(2\ell+1)P_\ell$ one can calculate the average value of ℓ from $\langle \ell(E) \rangle = \sum_\ell \ell\sigma_\ell / \sum \sigma_\ell$ and many other relevant quantities. Sometimes, for a better visualization, or for extrapolation to low energies, one uses the concept of *astrophysical S-factor*, redefining the cross section as

$$\sigma_F(E) = \frac{1}{E} S(E) \exp\left[-2\pi\eta(E)\right], \tag{2.2}$$

where $\eta(E) = Z_1 Z_2 e^2/\hbar v$, with v being the relative velocity. The exponential function is an approximation to $P_0(E)$ for a square-well nuclear potential plus Coulomb potential, whereas the factor $1/E$ is proportional to the area appearing in Eq. 2.1.

In order to use Eq. 2.1 one needs the nucleus-nucleus optical potential. This is badly known. It includes the effects of non-fusion channels, which might be hardly known. As it cannot be calculated from first principles, one adds an imaginary part to the real potential often without theoretical guidance. Except for few heroic attempts, theorists seem to have given up with it. Now

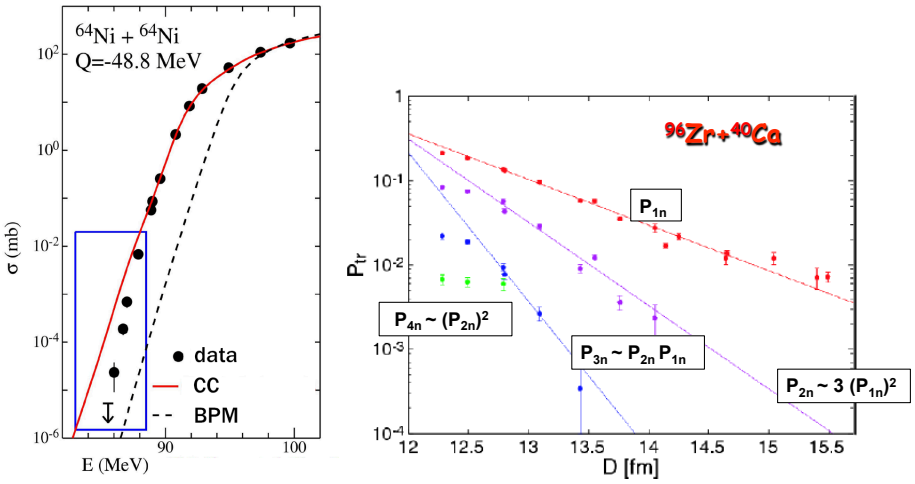

Figure 1: *Left* - Fusion cross section of ^{64}Ni+^{64}Ni as a function of the center of mass energy [25]. The dashed (solid) curve is a BPM (coupled-channel) calculation. *Right* - Transfer probabilities for multineutron transfer in ^{96}Zr+^{40}Ca (Courtesy L. Corradi).

we just fit whatever we can fit and we get whatever parameters of a potential function we can. Then we simply call it the “optical potential".

2.2 Many reaction channels

The situation is worse, as Eq. 2.1 does not work in most situations. A good example is shown in figure 1 (left), taken from Ref. [25]. Only by including coupling to other channels, the fusion cross sections can be reproduced. I will give here a time-dependent description of the time-dependent coupled-channels equations. Time can be replace by any other auxiliary variable.

Semiclassical coupled-channels equations. Consider $H = H_0 + V$, where H is the Hamiltonian composed by a non-perturbed Hamiltonian H_0 and a small perturbation V. The Hamiltonian H_0 satisfies an eigenvalue equation $H_0\psi_n = E_n\psi_n$, whose eigenfunctions form a complete basis in which the total wavefunction Ψ, that obeys the Schrödinger equation $H\Psi = i\hbar\partial\Psi/\partial t$, can be expanded:

$$\Psi = \sum_n a_n(t)\,\psi_n e^{-iE_nt/\hbar}. \tag{2.3}$$

Inserting this expansion in the Schrödinger equation, one obtains

$$i\hbar\sum_n \dot{a}_n\psi_n e^{-iE_nt/\hbar} = \sum_n Va_n\psi_n e^{-iE_nt/\hbar}, \tag{2.4}$$

with $\dot{a}_n \equiv da_n(t)/dt$. Using the orthogonalization properties of the ψ_n, we multiply (2.4) by ψ_k^* and integrate over the coordinate space to get the *coupled-channels equations*

$$\dot{a}_k(t) = -\frac{i}{\hbar}\sum_n a_n(t)\; V_{kn}(t)\; e^{i\frac{E_k-E_n}{\hbar}t}, \tag{2.5}$$

where the matrix element ($d\tau$ is the coordinate volume element) is $V_{kn} = \int \psi_k^* V \psi_n\, d\tau$.

Often, the perturbation V is very small and the system, initially in state $n = 0$, does not change appreciably. Thus we can insert $a_n = \delta_{n0}$ in the right-hand side of the equation 2.5, which yields

$$a_k(t) = \int_{-\infty}^{t} dt\ V_{k0}(t)\ e^{i(E_k - E_0)t/\hbar}. \tag{2.6}$$

This is the *first-order perturbation theory* result. Obtaining the coefficients a_n, the probability of occupation of state n is simply given by $|a_n(\infty)|^2$.

CDCC. In the presence of continuum states, continuum-continuum coupling (relevant for breakup channels) can be included by discretizing the continuum. This goes by the name of Continuum Discretized Coupled-Channels (CDCC) calculations. There are several variations of CC equations, e.g., a set of differential equations for the wavefunctions, instead of using basis amplitudes. One might use time-dependent discrete states defined as

$$\begin{aligned} &|\phi_b\rangle = e^{-iE_b t/\hbar}\,|b\rangle\,, \quad \text{for bound states} \\ &\text{and}\ \ \left|\phi_{jJM}\right\rangle = e^{-iE_j t/\hbar}\int \Gamma_j(E)\ |E, JM\rangle \quad \text{for continuum states,} \end{aligned} \tag{2.7}$$

where $|E, JM>$ are continuum wavefunctions of the projectile fragments (with or without the interaction with the target), with good energy and angular momentum quantum numbers E, JM. The functions $\Gamma_j(E)$ are assumed to be strongly peaked around an energy E_j in the continuum. Therefore, the discrete character of the states $\left|\phi_{jJM}\right\rangle$ (together with $|\phi_b\rangle$) allows an easy implementation of the coupled-states calculations. Calling them all together by $|\alpha\rangle$, the orthogonality of the discrete states 2.7 is guaranteed if $\int dE\ \Gamma_\alpha(E)\ \Gamma_\beta(E) = \delta_{\alpha\beta}$. Writing the time-dependent Schrödinger equation for $\Psi(t) = \sum_\alpha a_\alpha(t)\phi_\alpha$, taking the scalar product with the basis states and using orthonormality relations, we get the coupled-channels equations 2.5.

Coupled channels calculations with a large number of channels in continuum couplings, is one of the least controllable calculations. Anything can happen because of the phases of matrix elements: the couplings can add destructively or constructively, depending on the system and on the nuclear model. Such suppressions or enhancements are difficult to understand and need to be compared to other techniques for validation.

2.3 Direct capture reactions, e.g., radiative capture

For reactions involving light nuclei, only a few channels are of relevance. In this case, a real potential is enough for the treatment of fusion. For example, radiative capture cross sections of the type $n + x \to a + \gamma$ and πL ($\pi = E, (M)$ =electric (magnetic) L-pole) transitions can be calculated from (see, e.g., [26])

$$\sigma^{\rm d.c.}_{EL,J_b} = const. \times |\langle l_c j_c \|\mathscr{O}_{\pi L}\| l_b j_b\rangle|^2\,, \tag{2.8}$$

where $\mathscr{O}_{\pi L}$ is an EM operator, and $\langle l_c j_c \|\mathscr{O}_{\pi L}\| l_b j_b\rangle$ is a multipole matrix element involving bound (b) and continuum (c) wavefunctons. For electric multipole transitions ($\mathscr{O}_{\pi L} = r^L Y_{LM}$),

$$\langle l_c j_c \|\mathscr{O}_{EL}\| l_b j_b\rangle = const. \times \int_0^\infty dr\ r^L u_b(r) u_c(r), \tag{2.9}$$

where u_i are radial wavefunctions. The total direct capture cross section is obtained by adding all multipolarities and final spins of the bound state ($E \equiv E_{nx}$),

$$\sigma^{\rm d.c.}(E) = \sum_{L,J_b} (SF)_{J_b}\ \sigma^{\rm d.c.}_{L,J_b}(E)\ , \tag{2.10}$$

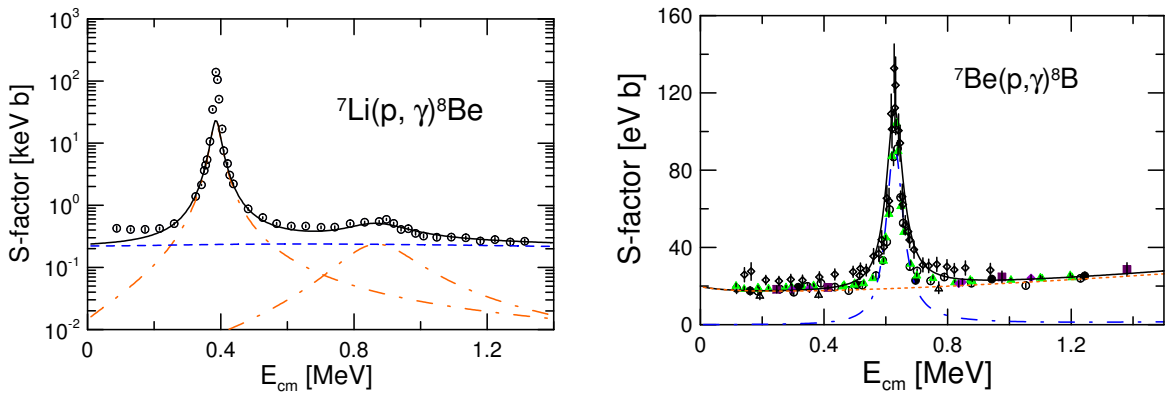

Figure 2: *Left.* - Potential model calculation for the reaction ^{7}Li (p, γ)^{8}Be. Experimental data are from Ref. [27]. *Right.* - Single-particle model calculations for the reaction $^7\mathrm{Be}(p,\gamma)^8\mathrm{B}$. The dashed-dotted line is the calculation for the M1 resonance at $E_{cm} = 0.63$ MeV and the dotted line is for the non-resonant capture. Experimental data are from Refs. [28, 29, 30, 31, 32, 33]. The total S factor is shown as a solid line.

where $(SF)_{J_b}$ are spectroscopic factors.

2.4 Asymptotic normalization coefficients

In a microscopic approach, instead of single-particle wavefunctions one often makes use of overlap integrals, $I_b(r)$, and a many-body wavefunction for the relative motion, $u_c(r)$. Both $I_b(r)$ and $u_c(r)$ might be very complicated to calculate, depending on how elaborated the microscopic model is. The variable r is the relative coordinate between the nucleon and the nucleus x, with all the intrinsic coordinates of the nucleons in x being integrated out. The direct capture cross sections are obtained from the calculation of $\sigma^{\mathrm{d.c.}}_{L,J_b} \propto |\left\langle I_b(r)||r^L Y_L||\Psi_c(r)\right\rangle|^2$.

The imprints of many-body effects will eventually disappear at large distances between the nucleon and the nucleus. One thus expects that the overlap function asymptotically matches ($r \to \infty$),

$$I_b(r) = C_1 \frac{W_{-\eta,l_b+1/2}(2\kappa r)}{r} \text{ for protons, } I_b(r) = C_2\sqrt{\frac{2\kappa}{r}} K_{l_b+1/2}(\kappa r) \text{ for neutrons,} \quad (2.11)$$

where the binding energy of the $n+x$ system is related to κ by means of $E_b = \hbar^2\kappa^2/2m_{nx}$, $W_{p,q}$ is the Whittaker function and K_μ is the modified Bessel function. In Eq. 2.11, C_i is the asymptotic normalization coefficient (ANC).

In the calculation of $\sigma^{\mathrm{d.c.}}_{L,J_b}$ above, one often meets the situation in which only the asymptotic part of $I_b(r)$ and $\Psi_c(r)$ contributes significantly to the integral over r. In these situations, $u_c(r)$ is also well described by a simple two-body scattering wave (e.g. Coulomb waves). Therefore the radial integration in $\sigma^{\mathrm{d.c.}}_{L,J_b}$ can be done accurately and the only remaining information from the many-body physics at short-distances is contained in the asymptotic normalization coefficient C_i, i.e. $\sigma^{\mathrm{d.c.}}_{L,J_b} \propto C_i^2$. We thus run into an effective theory for radiative capture cross sections, in which the constants C_i carry all the information about the short-distance physics, where the many-body aspects are relevant. It is worthwhile to mention that these arguments are reasonable for proton capture at very low energies, because of the Coulomb barrier.

As the overlap integral, Eq. 2.11, asymptotically becomes a Whittaker function, so does the single particle bound-state wavefunction u_α. If we call the single particle ANC by b_i, then the relation between the ANC obtained from experiment, or a microscopic model, with the single particle ANC is given by $(SF)_i b_i^2 = C_i^2$. This becomes clear from Eq. 2.10. The values of $(SF)_i$ and b_i obtained with the simple potential model are useful telltales of the complex short-range many-body physics of radiative capture reactions [26].

Many reactions of interest for nuclear astrophysics involve nuclei close to the dripline. To describe these reactions, a knowledge of the structure in the continuum is a crucial feature. One basic theoretical problem is to what extent we know the form of the effective interactions for threshold states. It is also hopeless that these methods can be accurate in describing high-lying states in the continuum. In particular, it is not worthwhile to pursue this approach to describe direct nuclear reactions.

2.5 Resonating group method

One immediate goal can be achieved in the coming years by using the Resonating Group Method (RGM) or the Generator Coordinate Method (GCM). These are a set of coupled integro-differential equations of the form

$$\sum_{\alpha'} \int d^3r' \left[H^{AB}_{\alpha\alpha'}(\mathbf{r},\mathbf{r}') - E N^{AB}_{\alpha\alpha'}(\mathbf{r},\mathbf{r}') \right] g_{\alpha'}(\mathbf{r}') = 0, \tag{2.12}$$

where $H^{AB}_{\alpha\alpha'}(\mathbf{r},\mathbf{r}') = \langle \Psi_A(\alpha,\mathbf{r}) | H | \Psi_B(\alpha',\mathbf{r}') \rangle$ and $N^{AB}_{\alpha\alpha'}(\mathbf{r},\mathbf{r}') = \langle \Psi_A(\alpha,\mathbf{r}) | \Psi_B(\alpha',\mathbf{r}') \rangle$. In these equations H is the Hamiltonian for the system of two nuclei (A and B) with the energy E, $\Psi_{A,B}$ is the wavefunction of nucleus A (and B), and $g_\alpha(\mathbf{r})$ is a function to be found by numerical solution of Eq. 2.12, which describes the relative motion of A and B in channel α. Full antisymmetrization between nucleons of A and B are implicit. Modern nuclear shell-model calculations, including the No-Core-Shell-Model (NCSM) are able to provide the wavefunctions $\Psi_{A,B}$ for light nuclei [24]. But the Hamiltonian involves an effective interaction in the continuum between the clusters A and B. Overlap integrals of the type $I_{Aa}(r) = \langle \Psi_{A-a} | \Psi_A \rangle$ for bound states has been calculated within the NCSM. This is one of the inputs necessary to calculate S-factors for radiative capture, $S_\alpha \sim |\langle g_\alpha | \mathscr{O}_{EM} | I_{Aa} \rangle|^2$, where $\mathscr{O}_{EM}$ is a corresponding electromagnetic operator. The left-hand side of this equation is to be obtained by solving Eq. 2.12. For some cases, in particular for the p+^{7}Be reaction, the distortion caused by the microscopic structure of the cluster does not seem to be crucial to obtain the wavefunction in the continuum. The wavefunction is often obtained by means of a potential model. The NCSM overlap integrals, I_{Aa}, can also be corrected to reproduce the right asymptotics [35, 36], given by $I_{Aa}(r) \propto W_{-\eta,l+1/2}(2k_0 r)$, where η is the Sommerfeld parameter, l the angular momentum, $k_0 = \sqrt{2\mu E_0}/\hbar$ with μ the reduced mass and E_0 the separation energy.

A step in the direction of reconciling structure and reactions for the practical purpose of obtaining astrophysical S-factors, along the lines described in the previous paragraph, was obtained in Ref. [35]. The wavefunctions obtained in this way were shown to reproduce very well the momentum distributions in knockout reactions of the type ^{8}B+$A \longrightarrow {}^7$Be+X. The astrophysical S-factor for the reaction ^{7}Be$(p,\gamma)^8$B was also calculated and excellent agreement was found with the experimental data in both direct and indirect measurements [35, 36]. The low- and high-energy

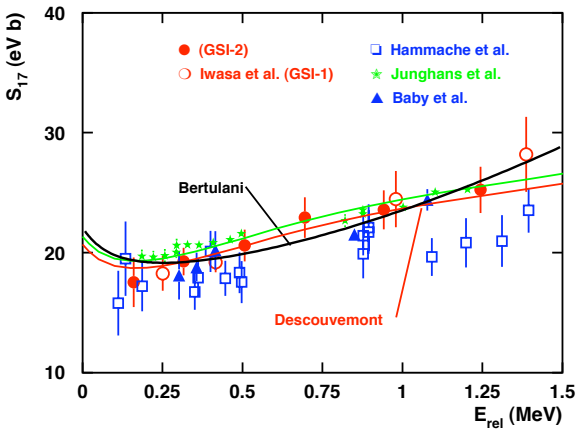

Figure 3: World data on ^{7}Be(p,γ)^{8}B compared to theoretical calculations.

slopes of the S-factor obtained with the NCSM is well described by the fit

$$S_{17}(E) = (22.109 \text{ eV.b}) \frac{1+5.30E+1.65E^2+0.857E^3}{1+E/0.1375}, \tag{2.13}$$

where E is the relative energy (in MeV) of p+^{7}Be in their center-of-mass. This equation corresponds to a Padé approximant of the S-factor. A subthreshold pole due to the binding energy of ^{8}B is responsible for the denominator [37, 38]. Figure 2.5 show the world data on ^{7}Be(p,γ)^{8}B compared to a few of the theoretical calculations. The recent compilation published in Ref. [22] recommends $S_{17} = 20.8 \pm 0.7$ (expt) ± 1.4 (theor) eV b.

3. Direct reactions and the role of radioactive beams

3.1 Coulomb excitation and Coulomb dissociation

Multipole expansions. Let us now consider a point particle with charge $Z_p e$ at a distance $\mathbf{r}$ from the center of a charge distribution where we put the origin of our frame of reference. At a point $\mathbf{r}'$ from the origin let the charge density be $\rho(\mathbf{r}')$. The potential created by the charge $Z_p e$ located at $\mathbf{r}$, averaged over the charge distribution, is

$$V_C(\mathbf{r}) = Z_p e \int d^3r' \frac{\rho(\mathbf{r}')}{|\mathbf{r}-\mathbf{r}'|} \approx \frac{Z_p Z_T e^2}{r} + \frac{\mathbf{p}\cdot\hat{\mathbf{r}}}{r^3} + \frac{Q_{ij} r_i r_j}{2r^5} + \cdots, \tag{3.1}$$

where $\mathbf{p} = \int \mathbf{r}'\rho(\mathbf{r}')d^3r'$ and $Q_{ij} = \int (3r'_i r'_j - r'^2)\rho(\mathbf{r}')d^3r'$ are the *dipole* and *quadrupole moments* of the charge distribution, respectively. In the last step we have expanded the factor $1/|\mathbf{r}-\mathbf{r}'|$ for $r \ll r'$, rearranged terms, and used $\int \rho(\mathbf{r}')d^3r' = Z_T e$. No big deal. Try deriving it yourself.

Semiclassical what?! In the semiclassical approximation, one assumes that the projectile's coordinate $\mathbf{r}$ can be replaced by $\mathbf{r}(t)$, following the classical trajectory of the projectile. The dependence on $\mathbf{r}'$ is used to treat $\mathbf{p}$ and Q_{ij} as operators. The excitation of nucleus T by nucleus P is obtained by using the matrix element $\langle f|V_C(\mathbf{r}',t)|i\rangle$, where $|i\rangle$ ($|f\rangle$) is initial (final) state of nucleus T. In

layperson's terms, it means the replacement of the static density $\rho(\mathbf{r}')$ by the *transition density* $\rho_{fi}(\mathbf{r}') = \Psi_f^*(\mathbf{r}')\Psi_i(\mathbf{r}')$ in Eq. 3.1, where Ψ_i (Ψ_f) is the initial (final) wavefunction of nucleus T.

The validity of the semiclassical approximation relies on the smallness of the wavelength $\lambda\!\!\!^{-} = \lambda/2\pi$ of the projectile's motion as compared to the distance of closest approach between the nuclei. Let us consider a central collision. The distance of closest approach is $a = 2a_0 = Z_P Z_T e^2/E$, where $E = mv^2/2$ is the kinetic energy of relative motion between the projectile and the target and m is the reduced mass. We can use the so-called *Sommerfeld parameter*, $\eta = a_0/\ \lambda\!\!\!^{-}$ to measure the validity of the semiclassical approximation. Since $\lambda\!\!\!^{-} = \hbar/p = \hbar/mv$, we have $\eta = Z_T Z_P e^2/mv \gg 1$ as the condition for validity of the semiclassical approximation. It is easy to verify that for nucleus-nucleus collisions this condition is valid for most cases of interest. In summary, the "*semi*" from semiclassical means "*quantum*". The "*classical*" means that the scattering part is treated in classical terms. The later is well justified in most situations.

Low energy central collisions. The fun part starts here. Consider the transition of the ground state $J = 0$ of a deformed nucleus to an excited state with $J = 2$ as a result of a frontal collision with scattering angle of $\theta = 180^\circ$. From Eq. 3.1 the perturbing potential is $V = \frac{1}{2} Z_p e^2 Q_{if}/r^3$. According to Eq. 2.6, the excitation amplitude to first order is

$$a_{if} = \frac{Z_p e^2 Q_{if}}{2i\hbar} \int \frac{e^{i\omega t}}{r^3}\, dt. \tag{3.2}$$

At an scattering of $\theta = 180^\circ$ a relationship exists between the separation r, the velocity v, the initial velocity v_0, given by $v = dr/dt = \pm v_0 (1 - a/r)^{1/2}$ (show this using energy conservation). If the excitation energy is small, we can assume that the factor $e^{i\omega t}$ in (3.2) does not vary much during the time that the projectile is close to the nucleus. The orbital integral is then solved easily by the substitution $u = 1 - a/r$, resulting in (you can do this integral, I know)

$$a_{if} = \frac{4 Z_p e^2 Q_{if}}{3i\hbar v_0 a^2} = \frac{4 Q_{if} E^2}{3 Z_p e^2 \hbar v_0 Z_T^2}. \tag{3.3}$$

The differential cross section is given by the product of the Rutherford differential cross section at 180° and the excitation probability along the trajectory, measured by the square of a_{if}. That is, $d\sigma/d\Omega|_{\theta=180^\circ} = d\sigma_R/d\Omega|_{\theta=180^\circ} \times |a_{if}|^2$. One obtains

$$\left.\frac{d\sigma}{d\Omega}\right|_{\theta=180^\circ} = \frac{m_0 E |Q_{if}|^2}{18\hbar^2 Z_T^2}, \tag{3.4}$$

where m_0 is the reduced mass of the projectile+target system. Oops! This expression is independent of the charge of the projectile. But you have always heard that heavy ions (large Z_P) are more efficient for Coulomb excitation. What is wrong? Show that there is nothing wrong.

General multipole expansion. Instead of Eq. 3.1, for electric excitations an exact multipole expansion can be carried out with the help of spherical harmonics:

$$V(\mathbf{r}) = \sum_{LM} \frac{4\pi}{2L+1} \frac{1}{r^{L+1}} Y_{LM}^*(\mathbf{r}) \mathscr{M}(EL, M). \tag{3.5}$$

The *electric multipole moment of rank* $L = 0, 1, \cdots$ is given by $\mathscr{M}(EL,M) = \int d^3r' \rho(\mathbf{r}') r'^L Y_{LM}(\mathbf{r}')$, where $M = -L, -L+1, ..., +L$.

In semiclassical calculations, $\mathbf{r}$ is replaced by a time-dependent coordinate along a Rutherford trajectory for the relative motion, $\mathbf{r}(t)$. As before, we can proceed to calculate the excitation amplitude for the transition of the target from a state with energy E_i to a state with energy E_f by replacing ρ by ρ_{if} (or $\mathscr{M}$ by $\mathscr{M}_{if}$) and integrating over time from $-\infty$ to $+\infty$. The cross section is obtained by squaring the excitation amplitude, summing it over final and averaging over the initial intrinsic angular momenta of the target. Oh, don't forget to multiply it by the Rutherford trajectory. One gets (with some omitted factors)

$$\frac{d\sigma_{EL}}{d\Omega} \simeq Z_P^2 \, B(EL) \, |I_{EL}(\omega_{fi})|^2, \tag{3.6}$$

where $\omega_{fi} = (E_f - E_i)/\hbar$ and $B(EL) \simeq \int dr' \, r'^L \rho_L(r')$ is the *reduced transition probability*. By the way, $\rho_L(r')$ is the radial part of the L-pole component of the transition density $\rho_{if}(\mathbf{r}')$. The factor I_{EL} involves a sum over M of the *orbital integrals* $I_{ELM}(\omega_{fi})$ given by

$$I_{ELM}(\omega_{fi}) = \int dt \, \frac{1}{r^{L+1}(t)} Y_{LM}\left(\hat{\mathbf{r}}(t)\right) e^{i\omega_{fi}t}. \tag{3.7}$$

Virtual photon numbers. Integration of (3.6) over all energy transfers $E_\gamma = E_f - E_i$, yields

$$\frac{d\sigma_C}{d\Omega} = \sum_{EL} \frac{d\sigma_{EL}}{d\Omega} = \sum_{EL} \int \frac{dE_\gamma}{E_\gamma} \frac{dn_{EL}}{d\Omega}(E_\gamma) \, \sigma_\gamma^{EL}(E_\gamma), \tag{3.8}$$

where σ_γ^{EL} are the *photonuclear cross sections*,

$$\sigma_\gamma^{EL}(E_\gamma) \simeq E_\gamma^{2L-1} \, B(EL) \, . \tag{3.9}$$

The *virtual photon numbers*, $n_{EL}(E_\gamma)$, are given by

$$\frac{dn_{EL}}{d\Omega}(E_\gamma) \simeq Z_p^2 \, |I_{EL}(E_\gamma)|^2. \tag{3.10}$$

The dependence of the cross section on the deflection angle is included in $dn_{EL}/d\Omega$. Since for a Rutherford trajectory the deflection angle is related to the impact parameter by $b = a_0 \cot\theta/2$, we can write the cross section in terms of an impact parameter dependence by using $dn_{EL}/2\pi b db \simeq \sin^4(\theta) dn_{EL}/d\Omega$.

The formalism above can be extended to treat magnetic multipole transitions, ML. It is much more complicated (involves currents, spins): hard work, but straight-forward.

The reactions induced by real photons include the contribution of all multipolarities with the same weight, i.e., $\sigma_\gamma(E_\gamma) = \sum_{E/M,L} \sigma_\gamma^{E/M,L}(E_\gamma)$, whereas according to Eq. 3.8, the excitation by virtual photons (e.g. Coulomb excitation) has different weights, $n_{E/M}$, for different multipolarities.

Figure 4 (left) shows the equivalent photon numbers per unit area, $dn_{EL}/2\pi b db$, incident on ^{208}Pb, in a collision with ^{16}O at 100 MeV/nucleon and with impact parameter $b = 15$ fm, as a function of the photon energy $E = \hbar\omega$. The curves for the E1, E2 and M1 multipolarities are shown. One sees that there is a cutoff for excitation energies beyond the adiabatic limit , i.e., $E_\gamma < \gamma\hbar v/b$. On the right we show the total number of virtual photons, $n_{EL} = \int_{b_{min}}^{\infty} db dn_{EL}/(2\pi b db)$, for the $E1$

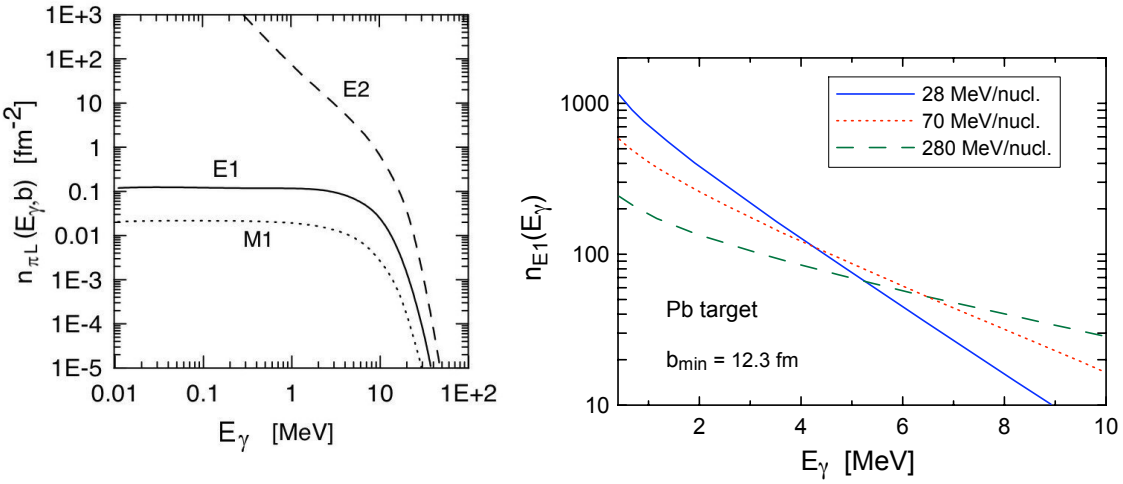

Figure 4: *Left:* Equivalent photon numbers per unit area incident on ^{208}Pb, in a collision with ^{16}O at 100 MeV/nucleon and with impact parameter $b = 15$ fm, as a function of the photon energy $E = \hbar\omega$. The curves for the E1, E2 and M1 multipolarities are shown. *Right:* Total number of virtual photons for the $E1$ multipolarity, "as seen" by a projectile passing by a lead target at impact parameters $b_{min} = 12.3$ fm and larger (i.e., integrated over impact parameters), for three typical bombarding energies.

multipolarity, "as seen" by a projectile passing by a lead target at impact parameters $b_{min} = 12.3$ fm and larger (i.e., integrated over impact parameters), for three typical bombarding energies. Lesson: more and more high energy photons are available as the beam energy increases.

We can easily understand the origin of the adiabatic condition by investigating the orbital integral, Eq. 3.7. Notice that for times larger than $t_{exc} = 1/\omega$ the integral oscillates too fast and I_{ELM} is small. For collisions at low energies, the collision time is given by $t_{coll} = a_0/v$, where $a_0 = Z_P Z_T e^2/2E_{c.m.}$. Thus, the excitation is possible if $t_{coll}/t_{exc} < 1$ otherwise the system will respond adiabatically (i.e. nothing interesting happens). This condition is called the *adiabatic condition*, $\omega a_0/v < 1$. For collisions at high energies, nuclei follow nearly straight-line orbits and it is more appropriate to use the impact parameter, b, as a measure of the distance of closest approach. The collision time is $t_{coll} = b/\gamma v$, where $\gamma = 1/\sqrt{1 - v^2/c^2}$ is the Lorentz contraction factor. Thus the adiabatic condition becomes $\omega b/\gamma v < 1$. Assuming an impact parameter of 20 fm, states with energy up to $\gamma\hbar v/(20\text{ fm})$ can be appreciably excited. Thus, even for moderate values of γ, i.e., $\gamma = 1 - 2$, it is possible to excite giant resonances. With increasing bombarding energies, ultraperipheral collisions can access the quasi-deuteron effect, produce deltas, mesons (e.g., J/Ψ), even the Higgs boson.

Nuclear response. The response function is

$$B(EL) \sim \left| \int r^L \rho_{if} d^3 r \right|^2 , \tag{3.11}$$

where $\rho_{if} = \Psi_f^* \Psi_i$ is the transition density. A simple estimate can be done for the excitation of high multipolarities by assuming that the wavefunctions have the form $\Psi_i = \Psi_f = 1/\sqrt{R^3}$, which yields $B(EL) \sim R^{2L}$, or, from Eq. 3.9, $\sigma_L^\gamma \sim (kR)^{2L}$, where $k = E_\gamma/\hbar c$. Thus, $\sigma_{L+1}/\sigma_L \sim (kR)^2$.

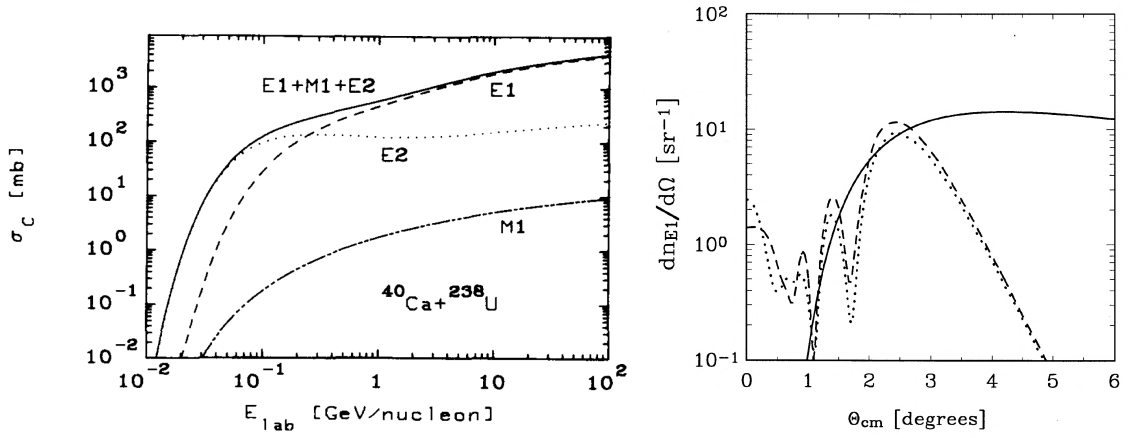

Figure 5: *Left:* Coulomb excitation cross section of giant resonances in ^{40}Ca projectiles hitting a ^{238}U target as a function of the laboratory energy per nucleon. The dashed line corresponds to the excitation of the giant electric dipole resonance, the dotted to the electric quadrupole, and the lower line to the magnetic dipole. The solid curve is the sum of these contributions. *Right:* Virtual photon numbers for the electric dipole multipolarity generated by 84A MeV ^{17}O projectiles incident on ^{208}Pb, as a function of the center-of-mass scattering angle. The solid curve is a semiclassical calculation. The dashed and dotted curves are eikonal calculations with and without relativistic corrections, respectively.

Usually $kR \ll 1$ (long-wavelength approximation) for low-lying states and we see that the cross sections decrease strongly with multipolarity.

It is useful to estimate the total photoabsorption cross section summed over all transitions $|i\rangle \rightarrow |f\rangle$. Such estimates are given by *sum rules* (SR) which approximately determine quantities of the following type: $\mathscr{S}[\mathscr{O}] = \sum_f (E_f - E_i)\left|\langle f|\mathscr{O}|i\rangle\right|^2$. Here the transition probabilities for an arbitrary operator $\mathscr{O}$ are weighted with the transition energy. For such *energy-weighted* sum rules (EWSR), $\mathscr{S}$, a reasonable estimate can be derived for many operators under certain assumptions about the interactions in the system. Using the completeness of the intermediate states, the commutation relations between the Hamiltonian and the operator $\mathscr{O}$, assuming that the Hamiltonian does not contain momentum-dependent interactions, one gets the EWSR for the dipole operator, $d_z = rY_{10}(\hat{\mathbf{r}})$, $\mathscr{S}[d_z] = \sum_a \hbar^2 e_a^2/2m_a$, where the sum extends over all particles with mass m_a and charge e_a.This is the old *Thomas-Reiche-Kuhn* (TRK) dipole SR.

We have to exclude the center-of-mass motion. Therefore our z-coordinates should be intrinsic coordinates, $z_a \Rightarrow z_a - R_z$, where $R_z = \sum_a z_a/A$. Hence, the intrinsic dipole moment is $d_z = \sum_a e_a(z_a - R_z) = e\sum_p z_p - (Ze/A)\left(\sum_p z_p + \sum_n z_n\right)$. This operator can be rewritten as $d_z = e_p\sum_p z_p + e_n\sum_n z_n$ where protons and neutrons carry *effective charges* $e_p = eN/A, \quad e_n = -eZ/A$. (Weird, no? Think about it.) This yields the *dipole EWSR*

$$\mathscr{S}[d_z] \equiv \sum_f E_{fi}|d_{fi}^z|^2 = \frac{\hbar^2 e^2}{2m_N}\frac{NZ}{A}, \tag{3.12}$$

where m_N is the nucleon mass. The factor (NZ/A) is connected to the reduced mass for relative motion of neutrons against protons as required at the fixed center of mass.

The EWSR (3.12) is what we need to evaluate the sum of dipole cross sections for real photons over all possible final states $|f\rangle$. Taking the photon polarization vector along the z-axis, we obtain the total dipole photoabsorption cross section

$$\sigma_{tot}^{\gamma} = \sum_f \int dE_\gamma \sigma_{fi}^{\gamma} = 2\pi^2 \frac{e^2\hbar}{m_N c} \frac{ZN}{A}. \tag{3.13}$$

This universal prediction on average agrees well with experiments in spite of crudeness of approximations made in the derivation. One should remember that it includes only dipole absorption. For the E2 isoscalar giant quadrupole resonances one can derive the approximate sum rule $\int dE_\gamma \sigma_{GQR}^{\gamma}(E_\gamma)/E_\gamma^2 \simeq 0.22 ZA^{2/3}\ \mu\text{b MeV}^{-1}$.

Resonances. A simple estimate of Coulomb excitation of giant resonances based on sum rules can be made by assuming that the virtual photon numbers vary slowly compared to the photonuclear cross sections around the resonance peak. Then

$$\sigma_C \simeq \frac{n_{E1}(E_{GDR})}{E_{GDR}} \int dE_\gamma \sigma_{GDR}^{\gamma}(E_\gamma) + n_{E2}(E_{GQR}) E_{GQR} \int \frac{dE_\gamma}{E_\gamma^2} \sigma_{GQR}^{\gamma}(E_\gamma). \tag{3.14}$$

In figure 5 we show the Coulomb excitation cross section of giant resonances in ^{40}Ca projectiles hitting a ^{238}U target as a function of the laboratory energy per nucleon. The dashed line corresponds to the excitation of the giant electric dipole resonance, the dotted to the electric quadrupole, and the lower line to the magnetic dipole which was also obtained using a sum-rule for M1 excitations [39]. The solid curve is the sum of these contributions. The cross sections increase very rapidly to large values, which are already attained at intermediate energies ($\sim$ 100 MeV/nucleon).

As with giant dipole resonances (GDR) in stable nuclei, one believes that *pygmy resonances* at energies close to the threshold are present in halo, or neutron-rich, nuclei. The *hydrodynamical model* predicts [40] for the width of the collective mode $\Gamma = \hbar\bar{\text{v}}/R$, where $\bar{\text{v}}$ is the average velocity of the nucleons inside the nucleus. This relation can be derived by assuming that the collective vibration is damped by the incoherent collisions of the nucleons with the walls of the nuclear potential well during the vibration cycles (*piston model*). Using $\bar{\text{v}} = 3\text{v}_F/4$, where $\text{v}_F = \sqrt{2E_F/m_N}$ is the Fermi velocity, with $E_F = 35$ MeV and $R = 6$ fm, one gets $\Gamma \simeq 6$ MeV. This is the typical energy width a giant dipole resonance state in a heavy nucleus. In the case of neutron-rich light nuclei $\bar{\text{v}}$ is not well defined. There are two average velocities: one for the nucleons in the core, $\bar{\text{v}}_c$, and another for the nucleons in the skin, or halo, of the nucleus, $\bar{\text{v}}_h$. Following Ref. [41], the width of momentum distributions of core fragments in knockout reactions, σ_c, is related to the Fermi velocity of halo nucleons by $\text{v}_F = \sqrt{5\sigma_c^2}/m_N$. Using this expression with $\sigma_c \simeq 20$ MeV/c, we get $\Gamma \simeq 1$ MeV, in accordance with experiments. Usually such modes are studied with the random phase approximation (RPA).

Eikonal waves. The free-particle wavefunction $\psi \sim e^{i\mathbf{k}\cdot\mathbf{r}}$ becomes "distorted" in the presence of a potential $V(\mathbf{r})$. The distorted wave can be calculated numerically by performing a partial wave-expansion solving the Schrödinger equation for each partial wave, i.e., if $\psi = \sum_{lm}(\chi_l(r)/r)Y_{lm}(\hat{\mathbf{r}})$, then

$$\left[\frac{d^2}{dr^2} + k_l^2(r)\right] \chi_l(r) = 0\,, \tag{3.15}$$

where

$$k_l(r) = \left\{ \frac{2\mu}{\hbar^2} \left[E - V(r) - \frac{l(l+1)\hbar^2}{2\mu r^2} \right] \right\}^{1/2} . \tag{3.16}$$

with the condition that asymptotically $\psi(\mathbf{r})$ behaves as a plane wave.

The solution of (3.15) involves a great numerical effort at large bombarding energies E. Fortunately, at large energies E a very useful approximation is valid when the excitation energies ΔE are much smaller than E and the nuclei (or nucleons) move in forward directions, i.e., $\theta \ll 1$. Calling $\mathbf{r} = (z, \mathbf{b})$, where z is the coordinate along the beam direction, we can assume that $\psi(\mathbf{r}) = e^{ikz}\phi(z, \mathbf{b})$, where ϕ is a slowly varying function of z and b, so that $\left|\nabla^2\phi\right| \ll k|\nabla\phi|$. In cylindrical coordinates the Schrödinger equation for ψ becomes

$$2ik\, e^{ikz}\frac{\partial\phi}{\partial z} + e^{ikz}\frac{\partial^2\phi}{\partial z^2} + e^{ikz}\nabla_b^2\phi - \frac{2m}{\hbar^2} V\, e^{ikz}\phi = 0$$

or, neglecting the 2nd and 3rd terms, we get $\partial\phi/\partial z = -iV(\mathbf{r})/\hbar \mathrm{v}\,\phi$, whose solution is

$$\phi = \exp\left\{ -\frac{i}{\hbar \mathrm{v}} \int_{-\infty}^{z} V(\mathbf{b}, z')dz' \right\}. \tag{3.17}$$

That is,

$$\psi(\mathbf{r}) = \exp\{ikz + i\chi(\mathbf{b}, z)\}. \tag{3.18}$$

This is the *eikonal function*, where

$$\chi(\mathbf{b}, z) = -\frac{1}{\hbar \mathrm{v}} \int_{-\infty}^{z} V(\mathbf{b}, z')dz' \tag{3.19}$$

is the *eikonal phase*. Given $V(\mathbf{r})$ one needs a single integral to determine the scattering wave.

Quantum scattering. Defining $\mathbf{r}$ as the separation between the center of mass of the two nuclei and $\mathbf{r}'$ as the intrinsic coordinate of the target nucleus, the inelastic scattering amplitude to first-order is given by [42]

$$f(\theta) = \frac{ik}{2\pi\hbar v} \int d^3r\, d^3r' \left\langle \Phi_{\mathbf{k}'}^{(-)}(\mathbf{r})\ \phi_f(\mathbf{r}') \ \middle|\ \mathscr{H}_{int}(\mathbf{r},\ \mathbf{r}') \ \middle|\ \Phi_{\mathbf{k}}^{(+)}(\mathbf{r})\ \phi_i(\mathbf{r}') \right\rangle, \tag{3.20}$$

where $\Phi_{\mathbf{k}'}^{(-)}(\mathbf{r})$ and $\Phi_{\mathbf{k}}^{(+)}(\mathbf{r})$ are the incoming and outgoing distorted waves, respectively, and $\phi(\mathbf{r}')$ is the intrinsic nuclear wavefunction of the target nucleus. Looks complicated. But that is the way we calculate quantum scattering amplitudes. Sometimes one calls this the Distorted Wave Born approximation (DWBA).

At intermediate energies, $\Delta E/E_{lab} \ll 1$, and forward angles, $\theta \ll 1$, we can use eikonal wavefunctions for the distorted waves. Corrections due to the extended nuclear charges can also be easily incorporated [42]. The results can also be cast in the form of Eq. 3.8. Trust me on this one.

In figure 5 we show the virtual photon numbers for the electric dipole multipolarity generated by 84A MeV ^{17}O projectiles incident on ^{208}Pb, as a function of the center-of-mass scattering angle. The solid curve is a semiclassical calculation. The dashed and dotted curves are eikonal calculations with and without relativistic corrections, respectively. One sees that the diffraction effects arising from the quantum treatment of the scattering change considerably the differential

cross sections. The corrections of relativity are also important. However, for small excitations both semiclassical and quantum scattering yield similar results for the differential cross section, as shown in figure 6 (left).

Intermediate energy Coulomb excitation. At low-energies, the theory of Coulomb excitation is very well understood [43]. A large number of small corrections are now well known in the theory and are necessary in order to analyze experiments on multiple excitation and reorientation effects. At the other end, the Coulomb excitation of relativistic heavy ions is characterized by straight-line trajectories with impact parameter b larger than the sum of the radii of the two colliding nuclei [45]. It was also shown that a quantum theory for relativistic Coulomb excitation leads to modifications of the semiclassical results [46]. The inclusion of relativistic effects in semiclassical and quantum formulations of Coulomb excitation was discussed in Refs. [48, 47]. Recently, the importance of relativistic effects in Coulomb excitation of a projectile by a target with charge Z_2, followed by gamma-decay, in nuclear reactions at intermediate energies was studied in details. In general terms, as we discussed above, the Coulomb excitation cross section is given by

$$\frac{d\sigma_{i\to f}}{d\Omega} = \left(\frac{d\sigma}{d\Omega}\right)_{\rm el} \frac{16\pi^2 Z_2^2 e^2}{\hbar^2} \sum_{\pi\lambda\mu} \frac{B(\pi\lambda, I_i \to I_f)}{(2\lambda+1)^3} \mid S(\pi\lambda,\mu) \mid^2, \tag{3.21}$$

where $B(\pi\lambda, I_i \to I_f)$ is the reduced transition probability of the projectile nucleus, $\pi\lambda = E1,\ E2,$ $M1,\ldots$ is the multipolarity of the excitation, and $\mu = -\lambda, -\lambda+1, \ldots, \lambda$.

The relativistic corrections to the Rutherford formula for $(d\sigma/d\Omega)_{\rm el}$ has been investigated in Ref. [44]. It was shown that the scattering angle increases by up to 6% when relativistic corrections are included in nuclear collisions at 100 MeV/nucleon. The effect on the elastic scattering cross section is even more drastic: up to 13% for center-of-mass scattering angles around 0-4 degrees.

The orbital integrals $S(\pi\lambda,\mu)$ contain the information about relativistic corrections. Inclusion of absorption effects in $S(\pi\lambda,\mu)$ due to the imaginary part of an optical nucleus-nucleus potential where worked out in Ref. [47]. These orbital integrals depend on the Lorentz factor $\gamma = (1 - v^2/c^2)^{-1/2}$, with c being the speed of light, on the multipolarity $\pi\lambda\mu$, and on the adiabacity parameter $\xi(b) = \omega_{fi} b/\gamma v < 1$, where $\omega_{fi} = (E_f - E_i)/\hbar$ is the excitation energy (in units of $\hbar$) and b is the impact parameter.

Ref. [49] has shown that at 10 MeV/nucleon the relativistic corrections are important only at the level of 1%. At 500 MeV/nucleon, the correct treatment of the recoil corrections is relevant on the level of 1%. Thus the non-relativistic treatment of Coulomb excitation [43] can be safely used for energies below about 10 MeV/nucleon and the relativistic treatment with a straight-line trajectory [45] is adequate above about 500 MeV/nucleon. However at energies around 50 to 100 MeV/nucleon, accelerator energies common to most radioactive beam facilities, it is very important to use a correct treatment of recoil and relativistic effects, both kinematically and dynamically. At these energies, the corrections can add up to 50%. These effects were also shown in Ref. [48] for the case of excitation of giant resonances in collisions at intermediate energies.

A reliable extraction of useful nuclear properties, like the electromagnetic response (B(E2)-values, γ-ray angular distribution, etc.) from Coulomb excitation experiments at intermediate energies requires a proper treatment of special relativity [49, 50]. The dynamical relativistic effects have often been neglected in the analysis of experiments elsewhere (see, e.g. [52]). The effect is highly non-linear, i.e. a 10% increase in the velocity might lead to a 50% increase (or decrease)

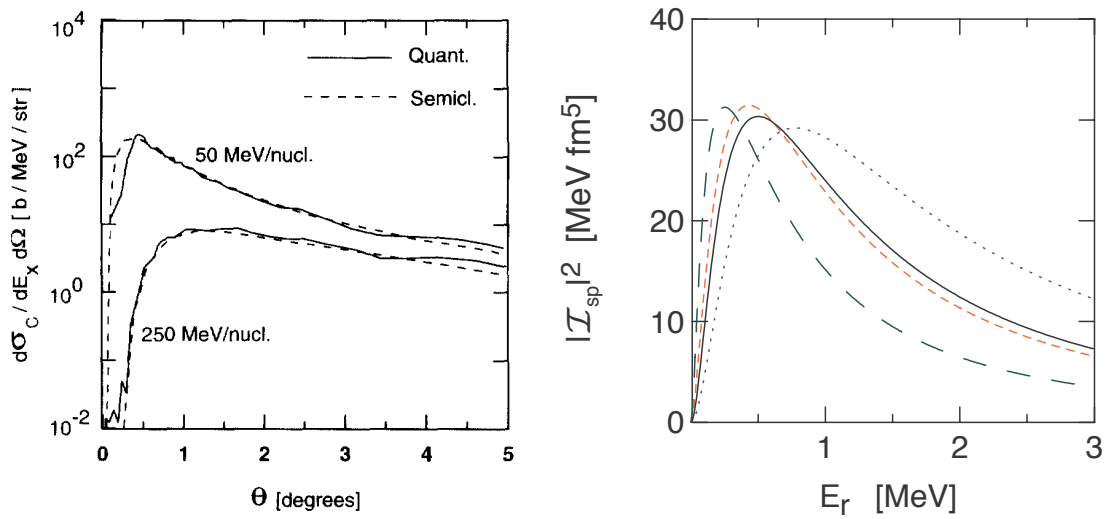

Figure 6: *Left:* Comparison of quantum (solid) and semiclassical (dashed) calculations of Coulomb excitation by $E_x = 1.5$ MeV of ^{8}B projectiles incident on lead at 50 and 250 MeV/nucleon, respectively. *Right:* Square of the integrals over coordinate, $\left|\mathscr{I}_{sp}\right|^2$, used in the calculation of the response function 3.11 in the single-particle model for a light, weakly-bound nucleus. Different scattering lengths and effective ranges were assumed for the final state.

of certain physical observables. A general review of the importance of the relativistic dynamical effects in intermediate energy collisions has been presented in Ref. [53, 51].

Single particle and collective response. Assume a loosely-bound particle described by an Yukawa of the form $\exp(-\eta r)/r$, where $\eta = \sqrt{2\mu_{bc}S}/\hbar$, μ_{bc} is the reduced mass of (particle b + core c), S is the separation energy. This is a reasonable assumption for the deuteron and also for other neutron *halo* systems. We further assume that the final state is a plane-wave state (i.e., we neglect final state interactions) $\psi_f \equiv \langle \mathbf{q}|\mathbf{r}\rangle = e^{i\mathbf{q}.\mathbf{r}}$. The response functions for electric multipole transitions, calculated from Eq. 3.11 is

$$\frac{dB(EL;E_\gamma)}{dE_\gamma} \sim \frac{\sqrt{S}(E_\gamma - S)^{L+1/2}}{E_\gamma^{2L+2}}. \tag{3.22}$$

The maximum of this function occurs at $E_0^{EL} = (L+\frac{1}{2})S/(L+\frac{3}{2}) \sim S$.

In figure 6 (right) we show a similar calculation as described above, but accounting for final state interactions in the form of scattering lengths and effective ranges (I wish I had more space to explain that, too.). The integrals over coordinate, denoted by $\mathscr{I}_{sp}$, show a strong dependence on the *final state interactions*. The strong dependence of the response function on the effective range expansion parameters makes it an ideal tool to study the scattering properties of light nuclei which are of interest for nuclear astrophysics.

The Coulomb dissociation method. As discussed above, the Coulomb breakup cross section for $a+A \to b+c+A$ can be written as

$$\frac{d\sigma_C^{\pi L}(E_\gamma)}{d\Omega} = N^{\pi L}(E_\gamma;\theta)\ \sigma^{\pi L}_{\gamma+a\,\to\,b+c}(E_\gamma), \tag{3.23}$$

where E_γ is the energy transferred from the relative motion to the breakup, and $\sigma^{\pi L}_{\gamma+a\,\to\,b+c}(E_\gamma)$ is the photo-dissociation cross section for the multipolarity πL and photon energy E_γ. Time reversal allows one to deduce the radiative capture cross section $b+c\to a+\gamma$ from $\sigma^{\pi L}_{\gamma+a\,\to\,b+c}(E_\gamma)$, i.e.,

$$\sigma_{b+c\to\,\gamma+a} = \frac{2(2j_a+1)}{(2j_b+1)(2j_c+1)}\frac{k_\gamma^2}{k^2}\sigma_{\gamma+a\,\to\,b+c}, \tag{3.24}$$

where $k_\gamma = E_\gamma/\hbar c$ is the photon wavenumber, and $k=\sqrt{2\mu(E_\gamma - B)}/\hbar$ is the wavenumber for the relative motion of b+c. Except for the extreme case very close to the threshold ($k\to 0$), we have $k_\gamma \ll k$, so that the phase space favors the photodisintegration cross section as compared to the radiative capture. Direct measurements of the photodisintegration near the break-up threshold do hardly provide experimental advantages and seem presently impracticable. On the other hand the copious source of virtual photons acting on a fast charged nuclear projectile when passing the Coulomb field of a (large Z) nucleus offers a way to study cross sections close to the breakup threshold.

This method was introduced in Ref. [54] and has been tested successfully in a number of reactions of interest to astrophysics. The most celebrated case is the reaction ^{7}Be$(p,\gamma)^8$B (see figure 2.5,). This reaction is important because it produces ^{8}B in the core of our sun. These nuclei decay by emitting high energy neutrinos which are one of the best probes of the sun's interior. The measurement of such neutrinos is very useful to test our theoretical solar models.

Schrödinger equation in a lattice. Another treatment of higher-order effects assumes solving the Schrödinger equation directly by discretizing space and time. This equation can be solved by a finite difference method assuming that the wavefunction can be expanded in several bound and unbound eigenstates $|\alpha\rangle$, as before. A truncation on the sum is obviously needed. To simplify, we discuss the method for one-dimensional problems. The wave function Ψ_α at time $t+\Delta t$ is obtained from the wave function at time t, according to the algorithm [55]

$$\Psi_\alpha(t+\Delta t) = \left[\frac{1}{i\tau} - \Delta^{(2)} + \frac{\Delta t}{2\hbar\tau}V_0\right]^{-1}\left[\frac{1}{i\tau} + \Delta^{(2)} - \frac{\Delta t}{2\hbar\tau}V_0 + \frac{\Delta t}{\hbar\tau}\,\widehat{S}\right]\Psi_\alpha(t). \tag{3.25}$$

In this equation $\tau = \hbar\Delta t/4\mu_{bx}(\Delta x)^2$ and $\widehat{S}\Psi_\alpha(t) = \sum_{\alpha'}\langle\alpha\,|V|\,\alpha'\rangle\,\Psi_{\alpha'}(t)$, with V being the time dependent potential, responsible for the transitions. V_0 is part of H_0.

The wave functions $\Psi_\alpha(x,t)$ are discretized in a mesh in space, with a mesh-size Δx. The second difference operator $\Delta^{(2)}$ is defined as $\Delta^{(2)}\Psi_\alpha^{(j)} = \Psi_\alpha^{(j+1)}(t) + \Psi_\alpha^{(j-1)}(t) - 2\Psi_\alpha^{(j)}(t)$, with $\Psi_\alpha^{(j)} \equiv \Psi_\alpha(r_j,t)$.

The wave function calculated numerically at a very large time will not be influenced by the Coulomb field. The numerical integration can be stopped there. The continuum part of the wave function is extracted by means of the relation (and normalized to unity)

$$\Psi_c(\mathbf{r},t) = \left[\Psi - \Psi_{gs} < \Psi_{gs}\,|\,\Psi>\right]\left[1 - |<\Psi_{gs}\,|\,\Psi>|^2\right]^{-1/2} \tag{3.26}$$

where Ψ_{gs} is the initial wave function. This wave function can be projected onto an (intrinsic) continuum state to obtain the excitation probability of the state.

Eikonal CDCC. To get quantum dynamical equations to treat higher-order effects, one discretizes the wavefunction in terms of the longitudinal center-of-mass momentum k_z, using the ansatz

$$\Psi = \sum_\alpha \mathscr{S}_\alpha(z,\mathbf{b})\ \exp(ik_\alpha z)\ \phi_{k_\alpha}(\xi). \tag{3.27}$$

In this equation, $(z,\mathbf{b})$ is the projectile's center-of-mass coordinate, with $\mathbf{b}$ equal to the impact parameter. $\phi(\xi)$ is the projectile intrinsic wavefunction and $(k,\mathbf{K})$ is the projectile's center-of mass momentum with longitudinal momentum k and transverse momentum $\mathbf{K}$.

Neglecting terms of the form $\nabla^2\mathscr{S}_\alpha(z,\mathbf{b})$ relative to $ik\partial_Z\mathscr{S}_\alpha(z,\mathbf{b})$, the Schrödinger (or the Klein-Gordon) equation reduces to

$$i\hbar v\frac{\partial\mathscr{S}_\alpha(z,\mathbf{b})}{\partial z} = \sum_{\alpha'}\langle\alpha|V|\alpha'\rangle\ \mathscr{S}_{\alpha'}(z,\mathbf{b})\ \mathrm{e}^{i(k_{\alpha'}-k_\alpha)z}. \tag{3.28}$$

These are the *eikonal-CDCC equations* (E-CDCC). They are much simpler to solve than the complicated low-energy CDCC equations because the z and b coordinates decouple and only the evolution on the z coordinate needs to be treated non-perturbatively. Of course, I lied and there are other complications (angular momentum coupling, etc.) hidden below the rug. If quantum field theorists can do it, why can't we?

The matrix element $\langle\alpha|V|\alpha'\rangle$ is Lorentz invariant. Boosting a volume element from the projectile to the laboratory frame means $d^3\xi \to d^3\xi/\gamma$. The intrinsic projectile wavefunction is a scalar and transforms according to $\phi_\alpha(\xi_x,\xi_y,\xi_z) \to \phi_\alpha(\xi_x,\xi_y,\gamma\xi_z)$, while V, treated as the time-like component of a four-vector, transforms as $V(b,z;\xi_x,\xi_y,\xi_z) \to \gamma V(b,z;\xi_x,\xi_y,\gamma\xi_z)$. Thus, redefining the integration variable z in the laboratory as $\xi_z' = \gamma\xi_z$ leads to the afore mentioned invariance. We can therefore calculate $\langle\alpha|V|\alpha'\rangle$ in the projectile frame.

The longitudinal wavenumber $\hbar k_\alpha c \simeq (E^2 - M^2c^4)^{1/2}$ also defines how much energy is gone into projectile excitation, since for small energy and momentum transfers $k'_\alpha - k_\alpha \sim (E'_\alpha - E_\alpha)/\hbar v$. In this limit, eq. 3.28 reduces to the semiclassical coupled-channels equations, Eq. 2.5, if one uses $z = vt$ for a projectile moving along a straight-line classical trajectory, and changing to the notation $\mathscr{S}_\alpha(z,b) = a_\alpha(t,b)$, where $a_\alpha(t,b)$ is the time-dependent excitation amplitude for a collision with impact parameter b.

3.2 Transfer reactions

Transfer reactions $A(a,b)B$ are effective when a momentum matching exists between the transferred particle and the internal particles in the nucleus. Thus, beam energies should be in the range of a few 10 MeV per nucleon. Low energy reactions of astrophysical interest can be extracted directly from breakup reactions $A+a \longrightarrow b+c+B$ by means of the Trojan Horse method (THM) [56]. If the Fermi momentum of the particle x inside $a = (b+x)$ compensates for the initial projectile velocity v_a, the low energy reaction $A+x = B+c$ is induced at very low (even vanishing) relative energy between A and x. To show this, one writes the DWBA cross section for the breakup reaction as

$$\frac{d^3\sigma}{d\Omega_b d\Omega_c dE_b} \propto \left|\sum_{lm} T_{lm}(\mathbf{k_a},\mathbf{k_b},\mathbf{k_c})S_{lx}Y_{lm}(\mathbf{k_c})\right|^2,$$

where

$$T_{lm} = < \chi_b^{(-)} Y_{lm} f_l | V_{bx} | \chi_a^+ \phi_{bx} > .$$

The threshold behavior E_x for the breakup cross section $\sigma_{A+x\to B+c} = (\pi/k_x^2)\sum_l (2l+1)|S_{lx}|^2$ is well known: since $|S_{lx}| \sim \exp(-2\pi\eta)$, then $\sigma_{A+x\to B+c} \sim (1/k_x^2)\ \exp(-2\pi\eta)$. In addition to the threshold behavior of S_{lx}, the breakup cross section is also governed by the threshold behavior of $f_l(r)$, which for $r \longrightarrow \infty$ is given by $f_{l_x} \sim (k_x r)^{1/2}\ \exp(\pi\eta)\ K_{2l+1}(\xi)$, where K_l denotes the Bessel function of the second kind of imaginary argument. The quantity ξ is independent of k_x and is given by $\xi = (8r/a_B)^{1/2}$, where $a_B = \hbar^2/mZ_AZ_xe^2$ is the Bohr length. From this one obtains that $(d^3/d\Omega_b d\Omega_c dE_b)(E_x \to 0) \approx$ const.. The coincidence cross section tends to a constant which will in general be different from zero. This is in striking contrast to the threshold behavior of the two particle reaction $A+x = B+c$. The strong barrier penetration effect on the charged particle reaction cross section is canceled completely by the behavior of the factor T_{lm} for $\eta \to \infty$. Basically, this technique extends the method of transfer reactions to continuum states. Very successful results using this technique have been reported [57, 58].

Another transfer method, coined as Asymptotic Normalization Coefficient (ANC) technique [59, 60, 61] relies on fact that the amplitude for the radiative capture cross section $b+x \longrightarrow a+\gamma$ is given by

$$M = < I^a_{bx}(\mathbf{r_{bx}}) | \mathscr{O}(\mathbf{r_{bx}}) | \psi_i^{(+)}(\mathbf{r_{bx}}) >,$$

where

$$I^a_{bx} = < \phi_a(\xi_b,\ \xi_x,\ \mathbf{r_{bx}}) | \phi_x(\xi_x)\phi_b(\xi_b) >$$

is the integration over the internal coordinates ξ_b, and ξ_x, of b and x, respectively. For low energies, the overlap integral I^a_{bx} is dominated by contributions from large r_{bx}. Thus, what matters for the calculation of the matrix element M is the asymptotic value of $I^a_{bx} \sim C^a_{bx}\ W_{-\eta_a,1/2}(2\kappa_{bx}r_{bx})/r_{bx}$, where C^a_{bx} is the ANC and W is the Whittaker function. This coefficient is the product of the spectroscopic factor and a normalization constant which depends on the details of the wave function in the interior part of the potential. Thus, C^a_{bx} is the only unknown factor needed to calculate the direct capture cross section. These normalization coefficients can be found from: 1) analysis of classical nuclear reactions such as elastic scattering [by extrapolation of the experimental scattering phase shifts to the bound state pole in the energy plane], or 2) peripheral transfer reactions whose amplitudes contain the same overlap function as the amplitude of the corresponding astrophysical radiative capture cross section.

To illustrate this technique, let us consider the proton transfer reaction $A(a,b)B$, where $a = b+p$, $B = A+p$. Using the asymptotic form of the overlap integral the DWBA cross section is given by

$$d\sigma/d\Omega = \sum_{J_B j_a} \left[\frac{(C^a_{Ap})^2}{\beta^2_{Ap}}\right]\left[\frac{(C^a_{bp})^2}{\beta^2_{bp}}\right]\tilde{\sigma}$$

where $\tilde{\sigma}$ is the reduced cross section not depending on the nuclear structure, β_{bp} (β_{Ap}) are the asymptotic normalization of the shell model bound state proton wave functions in nucleus $a(B)$ which are related to the corresponding ANC's of the overlap function as $(C^a_{bp})^2 = S^a_{bp}\beta^2_{bp}$. Here S^a_{bp} is the spectroscopic factor. Suppose the reaction $A(a,b)B$ is peripheral. Then each of the bound state wave functions entering $\tilde{\sigma}$ can be approximated by its asymptotic form and $\tilde{\sigma} \propto \beta^2_{Ap}\beta^2_{bp}$.

Hence $d\sigma/d\Omega = \sum_{j_i}(C^a_{Ap})^2(C^a_{bp})^2 R_{Ba}$ where $R_{Ba} = \tilde{\sigma}/\beta^2_{Ap}\beta^2_{bp}$ is independent of β^2_{Ap} and β^2_{bp}. Thus for surface reactions the DWBA cross section is actually parameterized in terms of the product of the square of the ANC's of the initial and the final nuclei $(C^a_{Ap})^2(C^a_{bp})^2$ rather than spectroscopic factors. This effectively removes the sensitivity in the extracted parameters to the internal structure of the nucleus. One of the many advantages of using transfer reaction techniques over direct measurements is to avoid the treatment of the screening problem [57, 61].

But do we really understand transfer reactions well enough? Using the first-Born approximation and a few corrections, the probability to transfer a nucleon in nucleus A from channel α to a nucleon in nucleus B in channel β is given by

$$P_{\beta\alpha} \sim \left| -i\hbar \int_{-\infty}^{\infty} dt F_{\beta\alpha}(\mathbf{R}) \exp\left[i\frac{E_\beta - E_\alpha)t}{\hbar} + (\cdots) \right] \right|^2, \tag{3.29}$$

where $\mathbf{R}$ is the nucleus-nucleus distance and $F_{\beta\alpha}(\mathbf{R})$ is the from factor given by

$$F_{\beta\alpha}(\mathbf{R}) = \int d^3 r e^{i\mathbf{Q}\cdot\mathbf{r}} \phi_\beta(\mathbf{R}+\mathbf{r}) \left(V_1 - \langle U \rangle\right) \phi_\alpha(\mathbf{r}), \tag{3.30}$$

where $\mathbf{Q}$ is the momentum transfer in the reaction, U is the total (optical) potential, and V_1 is the potential of the nucleon with one of the nuclei. Why not V_2? In the literature, using V_1 (V_2) goes by the name "prior" ("post)-form. It has been shown in the past that the post and prior forms of breakup and transfer reactions lead to the same result.

In figure 1 (right) one sees the probabilities for multinucleon transfer in ^{96}Zr+^{40}Ca, as a function of the closest approach distance $D = (Z_1 Z_2 e^2/2E)[1 + 1/\sin(\theta/2)]$. Transfer is most likely to occur when the nuclei are at their closest point, D. The tunneling probability depends exponentially on this distance, $P_{tr}/\sin(\theta/2) \sim \exp(-2\alpha D)$. This approximation arises from Eqs. 3.29 and 3.30. If one neglects correlations, two-nucleon transfer probabilities are given in terms one-nucleon transfer probabilities: $P_{2n} = (P_{1n})^2$. For three-nucleon transfer $P_{3n} = P_{1n}P_{2n}$, and so on. These are shown by the straight lines in figure 1 (Right). All seems to work well, except that one needs an enhancement of a factor 3 to get P_{2n} from theory [62]. That is what happens when theorists do not know what to do[1].

3.3 Charge exchange reactions

During core collapse, temperatures and densities are high enough to ensure that nuclear statistical equilibrium is achieved. This means that for sufficiently low entropies, the matter composition is dominated by the nuclei with the highest binding energy for a given Y_e. Electron capture reduces Y_e, driving the nuclear composition to more neutron rich and heavier nuclei, including those with $N > 40$, which dominate the matter composition for densities larger than a few 10^{10} g cm^{-3}. As a consequence of the model applied in collapse simulations, electron capture on nuclei ceases at these densities and the capture is entirely due to free protons. To understand the whole process it is necessary to obtain Gamow-Teller matrix elements which are not accessible in beta-decay experiments. Many-body theoretical calculations are right now the only way to obtain the required matrix elements. This situation can be remedied experimentally by using charge-exchange reactions. Charge exchange reactions induced in (p,n) reactions are often used to obtain values of

[1] Thanks to L. Corradi for reminding me of this

Gamow-Teller matrix elements, $B(GT)$, which cannot be extracted from beta-decay experiments. This approach relies on the similarity in spin-isospin space of charge-exchange reactions and β-decay operators. As a result of this similarity, the cross section $\sigma(\mathrm{p,n})$ at small momentum transfer q is closely proportional to $B(GT)$ for strong transitions [63],

$$\frac{d\sigma}{dq}(q=0) = KN_D|J_{\sigma\tau}|^2 B(\alpha), \tag{3.31}$$

where K is a kinematical factor, N_D is a distortion factor (accounting for initial and final state interactions), $J_{\sigma\tau}$ is the Fourier transform of the effective nucleon-nucleon interaction, and $B(\alpha = F, GT)$ is the reduced transition probability for non-spin-flip,

$$B(F) = (2J_i+1)^{-1}|\langle f||\sum_k \tau_k^{(\pm)}||i\rangle|^2,$$

and spin-flip,

$$B(GT) = (2J_i+1)^{-1}|\langle f||\sum_k \sigma_k\tau_k^{(\pm)}||i\rangle|^2,$$

transitions.

Eq. 3.31, valid for one-step processes, was proven to work rather well for (p,n) reactions (with a few exceptions). For heavy ion reactions the formula might not work so well. This has been investigated in refs. [64, 65, 66]. In Ref. [64] it was shown that multistep processes involving the physical exchange of a proton and a neutron can still play an important role up to bombarding energies of 100 MeV/nucleon. Refs. [65, 66] use the isospin terms of the effective interaction to show that deviations from the Taddeucci formula are common under many circumstances. As shown in Ref. [67], for important GT transitions whose strength are a small fraction of the sum rule the direct relationship between $\sigma(\mathrm{p,n})$ and $B(GT)$ values also fails to exist. Similar discrepancies have been observed [68] for reactions on some odd-A nuclei including ^{13}C, ^{15}N, ^{35}Cl, and ^{39}K and for charge-exchange induced by heavy ions [66, 69]. Undoubtedly, charge-exchange reactions such as (p,n), (^{3}He,t) and heavy-ion reactions (A,A$\pm$1) can provide information on the $B(F)$ and $B(GT)$ values needed for astrophysical purposes [70].

3.4 Knock-out reactions

Exotic nuclei are the raw materials for the synthesis of the heavier elements in the Universe, and are of considerable importance in nuclear astrophysics. Modern shell-model calculations are also now able to include the effects of residual interactions between pairs of nucleons, using forces that reproduce the measured masses, charge radii and low-lying excited states of a large number of nuclei. For very exotic nuclei the small additional stability that comes with the filling of a particular orbital can have profound effects upon their existence as bound systems, their lifetimes and structures. Thus, verifications of the ordering, spacing and the occupancy of orbitals are essential in assessing how exotic nuclei evolve in the presence of large neutron or proton imbalance and our ability to predict these theoretically. Such spectroscopy of the states of individual nucleons in short-lived nuclei uses direct nuclear reactions.

The early interest in knockout reactions came from studies of nuclear halo states, for which the narrow momentum distributions of the core fragments in a qualitative way revealed the large spatial

extension of the halo wave function. It was shown [71] that the longitudinal component of the momentum (taken along the beam or z direction) gave the most accurate information on the intrinsic properties of the halo and that it was insensitive to details of the collision and the size of the target. In contrast to this, the transverse distributions of the core are significantly broadened by diffractive effects and by Coulomb scattering. For experiments that observe the nucleon produced in elastic breakup, the transverse momentum is entirely dominated by diffractive effects, as illustrated [72] by the angular distribution of the neutrons from the reaction ^{9}Be(^{11}Be,^{10}Be+n)X. In this case, the width of the transverse momentum distribution reflects essentially the size of the target [73].

Most practical studies of medium corrections in nucleon-nucleon scattering are carried out by considering the effective two-nucleon interaction in infinite nuclear matter. This is known as the G-matrix method, an is obtained from a solution of the Bethe-Goldstone equation

$$\langle \mathbf{k}|\mathrm{G}(\mathbf{P},\rho_1,\rho_2)|\mathbf{k}_0\rangle = \langle \mathbf{k}|\mathrm{v}_{NN}|\mathbf{k}_0\rangle - \int \frac{d^3k'}{(2\pi)^3} \frac{\langle \mathbf{k}|\mathrm{v}_{NN}|\mathbf{k}'\rangle Q(\mathbf{k}',\mathbf{P},\rho_1,\rho_2)\langle \mathbf{k}'|\mathrm{G}(\mathbf{P},\rho_1,\rho_2)|\mathbf{k}_0\rangle}{E(\mathbf{P},\mathbf{k}') - E_0 - i\varepsilon}, \tag{3.32}$$

with $\mathbf{k}_0$, $\mathbf{k}$, and $\mathbf{k}'$ the initial, final, and intermediate relative momenta of the NN pair, $\mathbf{k} = (\mathbf{k}_1 - \mathbf{k}_2)/2$ and $\mathbf{P} = (\mathbf{k}_1 + \mathbf{k}_2)/2$. If energy and momentum is conserved in the binary collision, $\mathbf{P}$ is conserved in magnitude and direction, and the magnitude of $\mathbf{k}$ is also conserved. v_{NN} is the nucleon-nucleon potential. E is the energy of the two-nucleon system, and E_0 is the same quantity on-shell. Thus $E(\mathbf{P},\mathbf{k}) = e(\mathbf{P}+\mathbf{k}) + e(\mathbf{P}-\mathbf{k})$, with e the single-particle energy in nuclear matter. It is also implicit in Eq. 3.32 that the final momenta $\mathbf{k}$ of the NN-pair also lie outside the range of occupied states.

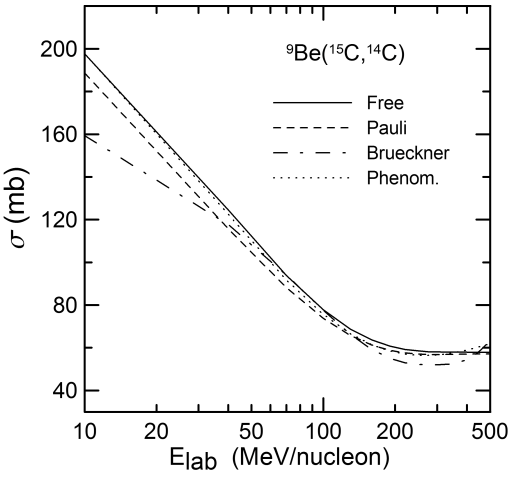

Figure 7: Total knockout cross sections for removing the $l = 0$ halo neutron of ^{15}C, bound by 1.218 MeV, in the reaction ^{9}Be(^{15}C,^{14}C$_{gs}$). The solid curve is obtained with the use of free nucleon-nucleon cross sections. The dashed curve includes the geometrical effects of Pauli blocking. The dashed-dotted curve is the result using the Brueckner theory, and the dotted curve is a phenomenological parametrization.

In Ref. [74] the numerical calculations have been performed to account for the geometric effect of Pauli blocking. A parametrization has been devised which fits the numerical results. The parametrization reads

$$\sigma_{NN}(E,\rho_1,\rho_2) = \sigma_{NN}^{free}(E) \frac{1}{1 + 1.892\left(\frac{2\rho_<}{\rho_0}\right)\left(\frac{|\rho_1-\rho_2|}{\tilde{\rho}\rho_0}\right)^{2.75}}$$

$$\times \begin{cases} 1-\frac{37.02\tilde{\rho}^{2/3}}{E}, & \text{if } E > 46.27\tilde{\rho}^{2/3} \\ \\ \frac{E}{231.38\tilde{\rho}^{2/3}}, & \text{if } E \leq 46.27\tilde{\rho}^{2/3} \end{cases} \tag{3.33}$$

where E is the laboratory energy in MeV, ρ_i is the local density of nucleus i, $\rho_< = \min(\rho_1, \rho_2)$ and $\tilde{\rho} = (\rho_1 + \rho_2)/\rho_0$, with $\rho_0 = 0.17$ fm^{-3}.

The Brueckner method goes beyond a treatment of Pauli blocking, and has been presented in several works, e.g. in Ref. [75, 76], where a simple parametrization was given, which we will from now on refer as Brueckner theory. It reads (the misprinted factor 0.0256 in Ref. [76] has been corrected to 0.00256)

$$\begin{aligned} \sigma_{np} &= \left[31.5 + 0.092\left|20.2 - E^{0.53}\right|^{2.9}\right] \frac{1 + 0.0034E^{1.51}\rho^2}{1 + 21.55\rho^{1.34}} \\ \sigma_{pp} &= \left[23.5 + 0.00256\left(18.2 - E^{0.5}\right)^{4.0}\right] \frac{1 + 0.1667E^{1.05}\rho^3}{1 + 9.704\rho^{1.2}} \end{aligned} \tag{3.34}$$

A modification of the above parametrization was done in Ref. [77], which consisted in combining the free nucleon nucleon cross sections parametrized in Ref. [78] with the Brueckner theory results of Ref. [75, 76].

To test the influence of the medium effects in nucleon knockout reactions, we consider the removal of the $l = 0$ halo neutron of ^{15}C, bound by 1.218 MeV, and the $l = 0$ neutron knockout from ^{34}Ar, bound by 17.06 MeV. The reaction studied is ^{9}Be(^{15}C,^{14}C$_{gs}$). The total cross sections as a function of the bombarding energy are shown in figures 7. The solid curve is obtained with the use of free nucleon-nucleon cross sections. The dashed curve includes the geometrical effects of Pauli blocking. The dashed-dotted curve is the result using the Brueckner theory, and the dotted curve is the phenomenological parametrization of the free cross section.

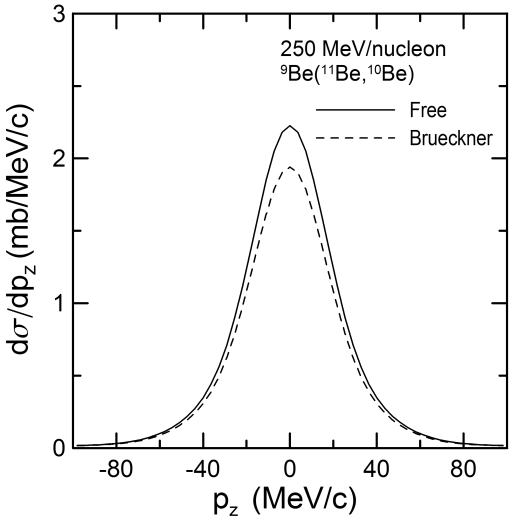

Figure 8: Longitudinal momentum distribution for the residue in the ^{9}Be(^{11}Be,^{10}Be), reaction at 250 MeV/nucleon. The dashed curve is the cross section calculated using the NN cross section from the Brueckner theory and the solid curve is obtained the free cross section.

In figure 8 we plot the longitudinal momentum distributions for the reaction ^{9}Be(^{11}Be,^{10}Be), at 250 MeV/nucleon [74]. The dashed curve is the cross section calculated using the NN cross section from the Brueckner theory and the solid curve is obtained with the free cross section. One sees that

the momentum distributions are reduced by 10%, about the same as the total cross sections, but the shape remains basically unaltered. If one rescales the dashed curve to match the solid one, the differences in the width are not visible [79].

References

[1] J.D. Lindl et al., The physics basis for ignition using indirect-drive targets on the National Ignition Facility, Phys. of Plasmas 11, 339 (2004).

[2] P. Monier-Garbet, Talk at the Fusion11 Conference, St. Malo, 2011. Private communication.

[3] C. A. Iglesias and F. J. Rogers, Astrophys. J. 464, 943 (1996).

[4] J.F. Hansen, S.G. Glendinning, R.F. Heeter, S.J. Brockington, Rev. Sci. Instrum. 79, 013504 (2008).

[5] Don Winget, private communication.

[6] J.N. Bahcall, Neutrino Astrophysics, (Cambridge: Cambridge University Press 1989).

[7] J. A. Frenje et al, Phys. Rev. Lett. 107, 122502 (2011).

[8] H.J. Assenbaum, K. Langanke and C. Rolfs, Z. Phys. A327 (1987) 461.

[9] C. Rolfs and E. Somorjai, Nucl. Inst. Meth. B99 (1995) 297.

[10] C. Rolfs, Prog. Part. Nucl. Phys. 46 (2001) 23.

[11] J. Kasagi et al., J. Phys. Soc. Jpn. 71, 277 (2002).

[12] K. Czerski et al., Europhys. Lett. 54, 449 (2001); Eur. Phys. J. A 27, 83 (2006).

[13] A.B. Balantekin, C.A. Bertulani, M.S. Hussein, Nucl. Phys. A627 (1997) 324.

[14] K. Langanke, T.D. Shoppa, C.A. Barnes and C. Rolfs, Phys. Lett. B369, 211 (1996).

[15] J.M. Bang, L.S. Ferreira, E. Maglione, and J.M. Hansteen, Phys. Rev. C53, R18 (1996).

[16] H. Andersen and J.F. Ziegler, “The Stopping and Ranges of Ions in Matter", Pergamon, NY, 1977.

[17] C.A. Bertulani and D.T. de Paula, Phys. Rev. C62 (2000) 045802.

[18] R. Golser and D. Semrad, Phys. Rev. Lett. 14, 1831 (1991).

[19] C.A. Bertulani, Phys. Let. B 585 (2004) 35.

[20] A. Formicola et al., Eur. Phys. J. A8, 443 (2000).

[21] L.S. Brown, and R. F. Sawyer, Astrophys. J. 489, 968 (1997).

[22] E.G. Adelberger et al., Rev. Mod. Phys. 83, 195 (2011).

[23] Nuclear Reactions with Heavy Ions, R. Bass, Springer Verlag, Berlin (2010). ISBN-10: 3642057187.

[24] Sofia Quaglioni and Petr Navrátil, Phys. Rev. Lett. 101, 092501 (2008).

[25] C.L. Jiang et al., Phys. Rev. Lett. 93 (2004) 012701.

[26] Junting Huang, C.A. Bertulani and V. Guimarães, Atomic Data and Nuclear Data Tables 96, 824 (2010).

[27] D. Zahnow et al, Z. Phys. A 351 229 (1995).

[28] F. J. Vaughn, R. A. Chalmers, D. Kohler and L. F. Chase, Phys. Rev. C 2, 1657 (1970).

[29] B. W. Filippone, A. J. Elwyn, C. N. Davids and D. D. Koetke, Phys. Rev.C 28, 2222 (1983).

[30] L. T. Baby et al., Phys. Rev. Lett. 90, 022501 (2003).

[31] A. R. Junghans et al, Phys. Rev. C 68, 065803 (2003).

[32] N. Iwasa et al., Phys. Rev. Lett. 83, 2910 (1999); B. Davids et al., ibid. 86, 2750 (2001); F. Schumann et al., ibid. 90, 232501 (2003).

[33] R.W. Kavanagh et al., Bull. Am. Phys. Soc. 14, 1209 (1969).

[34] P. Navratil, Phys. Rev. C. 70, 054324 (2004).

[35] P. Navratil, C.A. Bertulani, and E. Caurier, Phys. Lett. B 634 (2006) 191; Phys. Rev. C 73 (2006) 065801.

[36] Petr Navratil, Robert Roth, Sofia Quaglioni, Ab initio many-body calculation of the 7Be(p,gamma)8B radiative capture, arXiv:1105.5977.

[37] B. K. Jennings, S. Karataglidis, and T. D. Shoppa, Phys. Rev. C 58, 579 (1998).

[38] R. D. Williams and S. E. Koonin, Phys. Rev. C 23, 2773 (1981).

[39] C.A. Bertulani and G.Baur, *Phys. Reports* **163**, 299 (1988).

[40] W.D. Myers, et al., *Phys. Rev.* **C15**, 2032 (1977).

[41] C.A. Bertulani and K.W. McVoy, *Phys. Rev.* **C48**, 2534 (1993).

[42] C.A. Bertulani and P. Danielewicz, *Introduction to Nuclear Reactions*, IOP, London, 2004.

[43] K. Alder and A. Winther, Electromagnetic Excitation, North-Holland, Amsterdam, 1975.

[44] C.E.Aguiar, A.N.F.Aleixo and C.A.Bertulani, Phys. Rev. C 42, 2180 (1990).

[45] A. Winther and K. Alder, Nucl. Phys. A 319 (1979) 518.

[46] C.A.Bertulani and G.Baur, Phys. Reports 163 (1988) 299.

[47] C.A. Bertulani and A.M. Nathan, Nucl. Phys. A 554 (1993) 158.

[48] A.N.F. Aleixo and C.A. Bertulani, Nucl. Phys. A 505 (1989) 448.

[49] C.A. Bertulani, A. Stuchbery, T. Mertzimekis and A. Davies, Phys. Rev. C 68, 044609 (2003).

[50] C.A. Bertulani, C.M. Campbell, and T. Glasmacher, Comput. Phys. Commun. 152, 317 (2003).

[51] C.A.Bertulani, Phys. Rev. Lett. 94, 072701 (2005).

[52] T. Glasmacher, Nucl. Phys. A 693 (2001) 90.

[53] C.A. Bertulani, Proceedings of Workshop on "Reaction Mechanisms for Rare Isotope Beams" Michigan State University March 9-12,2005, arXiv.org:nucl-th/0505015.

[54] G. Baur, C. Bertulani and H. Rebel, Nucl. Phys. A459 (1986) 188.

[55] G.F. Bertsch and C.A. Bertulani, Nucl. Phys. A556 (1993) 136; Phys. Rev. C49 (1994) 2834; H. Esbensen, G.F. Bertsch and C.A. Bertulani, Nucl. Phys. A581 (1995) 107.

[56] G. Baur, Phys. Let. B178 (1986) 135.

[57] M. La Cognata et al., Phys. Rev. C 76, 065804 (2007).

[58] R.G. Pizzone et al, Few-Body Systems 50, 319 (2011).

[59] A.M. Mukhamedzhanov and N.K. Timofeyuk, JETP Lett. 51, 282 (1990).

[60] R.E. Tribble et al., Proceedings of Science (online at: http://pos.sissa.it/index.html), 2007.

[61] A.M. Mukhamedzhanov et al, J. Phys. Conference Series 202, 012017 (2010).

[62] R. Künkel et al., Z. Phys. A 336 (1990) 71.

[63] T.N. Tadeucci et al., Nucl. Phys. A469 (1987) 125.

[64] H. Lenske, H.H. Wolter and H.G. Bohlen, C.A. Bertulani, Phys. Rev. Lett. 62, 1457 (1989).

[65] C.A. Bertulani, Nucl. Phys. A 554 (1993) 493.

[66] C.A. Bertulani and P. Lotti, Phys. Lett. B 402 (1997) 237; C.A. Bertulani and D. Dolci, Nucl. Phys. A674 (2000) 527.

[67] S.M. Austin, N. Anantaraman and W.G. Love, Phys. Rev. Lett. 73 (1994) 30.

[68] J.W. Watson et al., Phys. Rev. Lett. 55 (1985) 1369.

[69] M. Steiner, et al., Phys. Rev. Lett. 76 (1996) 26.

[70] H. Fujita et al, Phys.Rev. C 79, 024314 (2009)

[71] C. A. Bertulani and K. W. McVoy, Phys. Rev. C 46, 2638 (1992).

[72] R. Anne, et al., Nucl. Phys. A 575 (1994) 125.

[73] C. A. Bertulani and P. G. Hansen, Phys. Rev. C 70, 034609 (2004).

[74] C.A. Bertulani and C. De Conti, Phys. Rev. C 81, 064603 (2010).

[75] G. Q. Li and R. Machleidt, Phys. Rev. C 48, 1702 (1993).

[76] G. Q. Li and R. Machleidt, Phys. Rev. C 49, 566 (1994).

[77] Cai Xiangzhou, Feng Jun, Shen Wenqing, Ma Yugang, Wang Jiansong, and Ye Wei, Phys. Rev. C58, 572 (1998).

[78] S. K. Charagi and S. K. Gupta, Phys. Rev. C 41, 1610 (1990).

[79] M. Karakoç et al (2011), in preparation.